

Two-stream ballistic instability and terahertz oscillation generation in n^+nn^+ - ballistic diodes and field-effect transistors

Z. S. Gribnikov, N. Z. Vagidov, and V. V. Mitin

Department of Electrical and Computer Engineering, Wayne State University,
Detroit, Michigan 48202, USA

I. Introduction

Two groups of current carriers naturally coexist in the quasineutral regions (QRs) of the base of ballistic diodes and field-effect transistors (FETs). They are (Fig.1): 1.

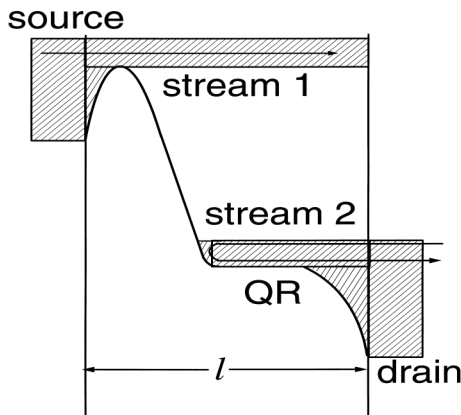


Fig.1. Two streams in a ballistic diode: 1 — traversing ballistic carriers, 2 — nontraversing carriers being in the equilibrium with the drain reservoir.

2. nontraversing (nonparticipating in a current flow) carriers, which are in the equilibrium with the drain current reservoir. As a result of interactions between these carrier streams a two-stream instability appears and develops in such diodes and FETs if they have appropriate material and geometrical parameters.

The 2-stream instability (2-SI) goes back to the pioneer works of J.R. Pierce [1]. It appears both in gas discharge plasmas and solid state plasmas if these plasmas contain two (or more) mobile components with different directional drift velocities. In the 60-s the 2-SI in electron-hole plasma of bulk InSb was adjusted for description of K-band coherent microwave

radiation [2,3]. V.I. Ryzhii and his co-authors [4,5] first paid attention to the 2-SI manifestations in ballistic and quasiballistic electron transport for short-base n^+nn^+ -diodes.

The 2-SI is a result of collective plasma oscillations of both above-mentioned carrier groups. In this work we study analytically dispersion relations for the 2-SI in the QRs of the ballistic diodes and FETs and consider numerically development of this instability in the short-base diodes and FETs.

II. Two-stream instability

The dispersion equation for plasma oscillations in the QR of the bulk base diode has conventional form for the model cold stream in cold plasma [6]:

$$\frac{\omega_1^2}{(\omega(k) - kv)^2} + \frac{\omega_2^2}{\omega^2(k)} = 1 \quad (1)$$

where $\omega_{1,2}$ are the plasma frequencies of electrons in the streams 1 and 2 (Fig.1):

$$\omega_{1,2}^2 = e^2 n_{1,2} / \kappa_D m_{1,2}, \quad (2)$$

v is an electron velocity in the stream 1. For the parabolic dispersion relations we have in the QR not only $m_1 = m_2 = m$, but also $n_1 = n_2 = n_0/2$. Therefore: $\omega_1^2 = \omega_2^2 = \omega_0^2/2$ and we obtain from Eq. (1):

$$\omega_{(1,2,3,4)}(k) = (1/2) \left\{ kv \pm \left[k^2 v^2 + 2\omega_0^2 \pm 2(\omega_0^4 + 2k^2 v^2 \omega_0^2)^{1/2} \right] \right\}. \quad (3)$$

The instability occurs if

$$|kv| < 2 \omega_0. \quad (4)$$

In accordance with [6] this instability is always convective. Current oscillations appear as a result of globalization of this instability in the globalization of the finite (short-base!) diodes with shorted (or terminated in a sufficiently small resistance) drain and source.

The condition of Eq. (4) means that the considered instability can occur only for sufficiently low voltages across the diode. Since $k_{\min} \sim 2\pi/l'$ (l' is a length of the QR) we can obtain

$$v_{\max} = \sqrt{\frac{2eV_{\max}}{m}} \cong \frac{\omega_0}{\pi} l' \quad (5)$$

and $V_{\max} \cong en_0 l'^2 / 2\pi^2 \kappa_D$, where n_0 is a donor concentration. The maximal frequency is of order ω_0 and does not depend on the length l' . We are interested in high electron concentrations and in small masses to raise ω_0 .

For the top- and bottom-gated n -channel base (Fig.2), that is for the FET (with 2 gates) the dispersion equation, which is analogous to Eq. (1), has a form:

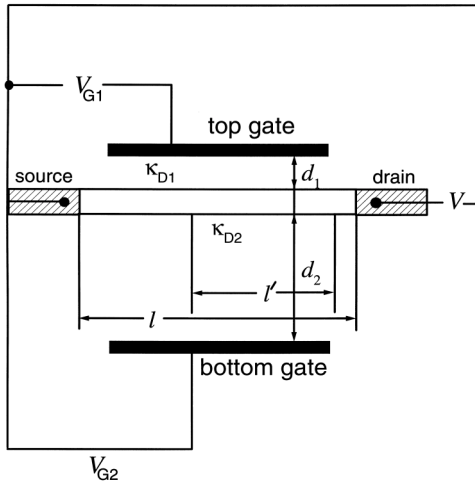


Fig.2. Gated ballistic diode (ballistic FET). Symmetric version: $d_1 = d_2 = d$; $\kappa_{D1} = \kappa_{D2}$. Asymmetric version: $\kappa_{D1} = \kappa_{D2}$; $d_1 = d$; $d_2 =$

$$\frac{g_1 k}{(\omega(k) - kv)^2} + \frac{g_2 k}{\omega^2(k)} = \frac{\kappa_{D1}}{\tanh kd_1} + \frac{\kappa_{D2}}{\tanh kd_2}, \quad (6)$$

where $g_{1,2} = e^2 N_{1,2} / m_{1,2}$, and $N_{1,2}$ are sheet electron concentrations of the 1 and 2 groups (streams) in the channel; $m_{1,2}$ are their effective masses. For the parabolic electron dispersion, $m_1 = m_2$, but now $N_1 \neq N_2$ (unlike the bulk base case). This is because the gate potentials $V_{G1,2}$ (see Fig. 2) govern the full channel concentration $N = N_1 + N_2$ mainly by taking from the concentration N_2 of only immobile electrons. The mobile (traversing!) electrons carry the current, and this current determines their concentration N_1 . The concentration N_2 depends on $V_{G1,2} - V$, where V is the potential of the QR and for a certain value of $V = V_S$ we have $N_2 = 0$, and the current saturates. Of course we have no 2-SI in the saturated regime because of absence of the second stream. But for $V < V_S$ we have both streams with $N_2 < N_1$, and the 2-SI is possible. This instability for the ballistic FETs was discovered by Sukhanov with coauthors [7,8].

In a symmetrical case, when $d_1 = d_2 = d$, $\kappa_{D1} = \kappa_{D2} = \kappa_D$, Eq. (6) transforms to:

$$\frac{G_1}{(\omega(k) - kv)^2} + \frac{G_2}{\omega^2(k)} = \frac{1}{k \tanh kd}, \quad (7)$$

where $G_{1,2} = e^2 N_{1,2} / 2 \kappa_D m$. In an asymmetrical case, when $d_1 = d$, $\kappa_{D1} = \kappa_{D2} = \kappa_D$, $d_2 \rightarrow \infty$, and we obtain

$$\frac{G_1}{(\omega(k) - kv)^2} + \frac{G_2}{\omega^2(k)} = \frac{1}{2k \tanh kd} + \frac{1}{2|k|}. \quad (8)$$

In a case of the ungated channel ($d_1, d_2 \rightarrow \infty$) we have the asymptotic formula with $1/|k|$ on the right-hand side of Eq. (8). Due to existence of $\tanh kd$ on the right-hand sides of Eqs. (7) and (8) the instability changes its type: it becomes absolute (instead of convective).

The numerical calculations (see below) show that the result of this absolute instability is stratification of the sheet concentration in the conducting channel of the FET. This stratification depends on the concentration (N) and the gate-channel distance (d). If an amplitude of the stratification and its spatial period are small, this stratification does not impede development of oscillatory regime. It seems that there appears convective instability of the anew formed stratified stationary state. As a result of this secondary convective instability, we obtain the same current oscillations and terahertz radiation. But if the amplitude and spatial period of electron concentration strata are large, the anew formed state is stable and we can not obtain oscillatory regime.

The main problem which must be solved to implement 2-SI terahertz generators is blocking pair electron-electron interactions between electrons from different streams (groups). We have to protect their collective plasma interaction and to avoid their pair (fluctuative) interaction (scattering). This scattering leads to energy and momentum exchange and transforms two streams into a single united stream (see, for example, [9]). As a result we lose the 2-SI. To avoid this undesirable fact we suggest to reconstruct a

design of ballistic FET: to replace metallic gates by semiconductor gates with electron concentration which is approximately equal to the concentration $N_I = N$ of mobile (traversing) carriers in the main channel at saturation regime. This design allows obtaining a certain FET structure with mobile (traversing) electrons only in the main channel (the 1-st stream) and with immobile electrons in the additional channel (that is, in the semiconductor gate). These nontraversing electrons form the 2-nd stream. Plasma interaction between streams occurs across the barrier layer of width d , and it is effective for $kd < 1$. If $l' \gg d$ this interaction is sufficiently effective for all actual k . The range of pair scattering is short and can be suppressed (similarly to the well-known suppression of electron-ion scattering by the modulation doping). The dependence of the interlayer electron-electron scattering on the distance d was considered in great detail (see [10] and references therein). The inverse characteristic time τ_D^{-1} of this scattering decreases with d at least as d^{-4} .

The simplest dispersion equation describing the studied two-stream interaction for the considered two-channel structure (Fig.3) has the form (for the saturated regime):

$$\frac{G_I}{(\omega(k) - kv)^2} + \frac{G_{II}}{\omega^2(k)} = \frac{\tanh kd}{k} \left(1 + \frac{k^2 G_I G_{II}}{(\omega(k) - kv)^2 \omega^2(k)} \right), \quad (10)$$

where $G_{I,II} = e^2 N_{I,II} / 2\kappa_D m_{I,II}$, and indexes I and II relate to the main and the additional channels, respectively. Voltages V_D and V_G (see Fig.3) redistribute concentration N_I and N_{II} . Only their sum $N = N_I + N_{II}$ is constant and is determined by the summary doping. For $kd \ll 1$ the complex conjugate roots of Eq. (10) have the approximate form:

$$\omega_{(1,2)}(k) \cong k\sqrt{\bar{G}d} \sqrt{1 - \left(\frac{\delta G}{\bar{G}}\right)^2} \left(\sqrt{1 - \left(\frac{\delta G}{\bar{G}}\right)^2} \pm i \sqrt{3/2 + \left(\frac{\delta G}{\bar{G}}\right)^2} \right), \quad (11)$$

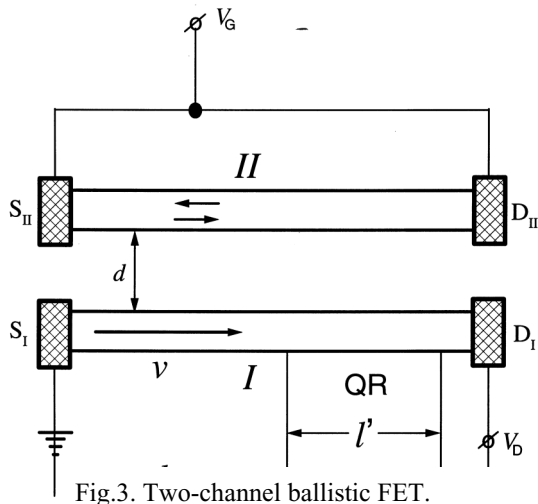


Fig.3. Two-channel ballistic FET.

where $\bar{G} = \frac{1}{2}(G_I + G_{II})$, $\delta G = \frac{1}{2}(G_I - G_{II})$, and the instability disappears only if $G_I = 0$ or $G_{II} = 0$. For presaturated regimes in such structures three different streams (groups) of electrons participate in plasma oscillations: mobile electrons in channel I and immobile electrons from both channel II and channel I, and we deal with three-stream oscillations.

III. Numerical results

IV-characteristics for 5 different samples

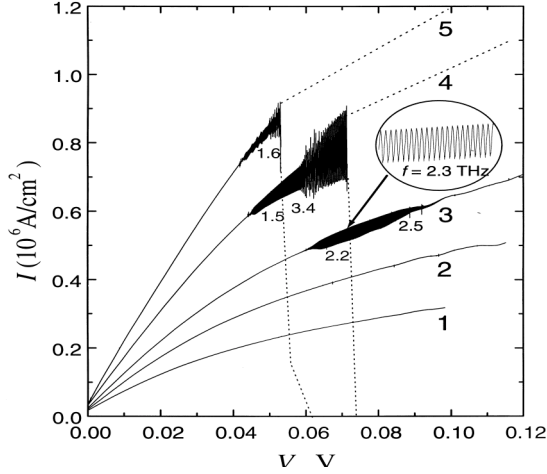


Fig.4. IV-characteristics of n^+nn^+ -ballistic diodes. Parameters: $T = 30$ K, $l = 0.15$ μm , $m = 0.067m_0$, $\mu_F = 0.025$ eV, $n_0 = 5 \cdot 10^{16}$ cm^{-3} (1), $7.5 \cdot 10^{16}$ cm^{-3} (2), 10^{17} cm^{-3} (3), $1.5 \cdot 10^{17}$ cm^{-3} (4), $2 \cdot 10^{17}$ cm^{-3} (5).

of current oscillation amplitudes. The frequencies of oscillations (in THz) are indicated alongside the characteristics. Distributions of the oscillating electron concentration in the n^+nn^+ -ballistic diode base (with $n_0 = 10^{17}$ cm^{-3}) are shown in Fig. 5. Time interval between each neighboring curves is 0.75 ps. We see a certain travelling wave in the QR and an almost standing oscillation in the depletion layer.

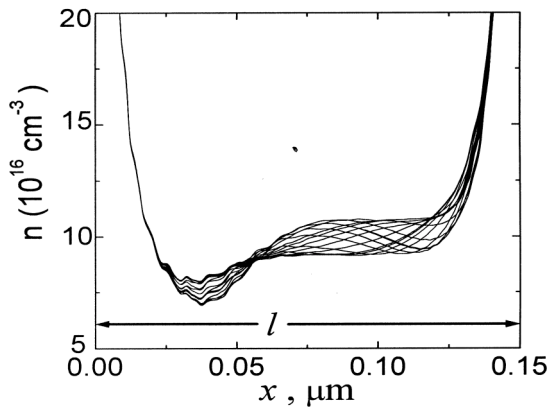


Fig.5. Snapshots of concentration distribution n in sample 3 from Fig.4. Applied voltage is 0.075 V.

in wide ranges.

of n^+nn^+ -ballistic diodes with quasibulk material bases are shown in Fig.4. The quasibulk material is formed of 2D-electrons (with a parabolic dispersion in plane) tightly stacked to each other without any clearance. Such a material differs from a real 3D-bulk material only in the density of states. All of these bases are of the length $l = 0.15$ μm , which allows us to consider electron transport for voltages up to 0.12 V as quasiballistic. The samples with $n_0 < 10^{17}$ cm^{-3} do not display any current oscillations. The samples with $n_0 \gtrsim 10^{17}$ cm^{-3} demonstrate oscillations initiated by the 2-SI. For the samples with $n_0 \gtrsim 1.5 \cdot 10^{17}$ cm^{-3} Fermi energy $\mu_F = 0.025$ eV selected for source and drain contacts is insufficient to keep the effective cathode regime. Therefore N-shaped IV-characteristics appear. It leads to explosion

The same as in Fig. 4 oscillation portraits but for three FETs with a single gate ($d_2 = \dots$) and with quantized electrons in the channels are shown in Fig. 6. The presented samples are of the same parameters (doping, gate potential, Fermi-energies of electrons in the drain and source, etc.) but they differ from each other in the gated base length. We see that oscillations are more intensive in the longer samples but the maximal frequency is in the shortest of them. Dependences of oscillation amplitudes and frequencies on gate potentials V_G are shown in Figs. 7 and 8. We see both smooth frequency tuning and sharp variations. In both cases gate potential V_G changes oscillation frequency

Figure 9 demonstrates development of absolute instability in asymmetric gated ballistic FET with extended distance channel-gate ($d = 0.048 \mu\text{m}$). As a result of this extension, the amplitude of concentration stratification is very high and a period of strata is also large. This stratification impedes oscillation regime, but it is not displayed here.

This work is supported by NSF.

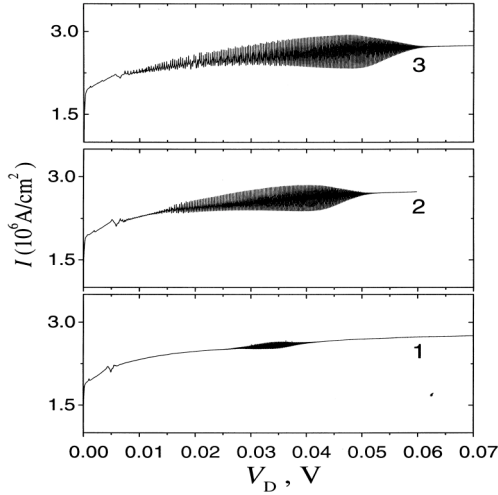


Fig.6. IV-characteristics of asymmetric ballistic FETs of different base lengths l : 0.125 μm (1), 0.15 μm (2), 0.175 μm (3). Fermi-energies of source-contact $\epsilon_F^{(S)} = 0.06 \text{ eV}$ and drain-contact $\epsilon_F^{(D)} = 0.015 \text{ eV}$; $V_G = -0.03 \text{ V}$, $N_0 = 4 \cdot 10^{11} \text{ cm}^{-2}$, $d = 0.016 \mu\text{m}$. Other parameters are the same as in Fig.4.

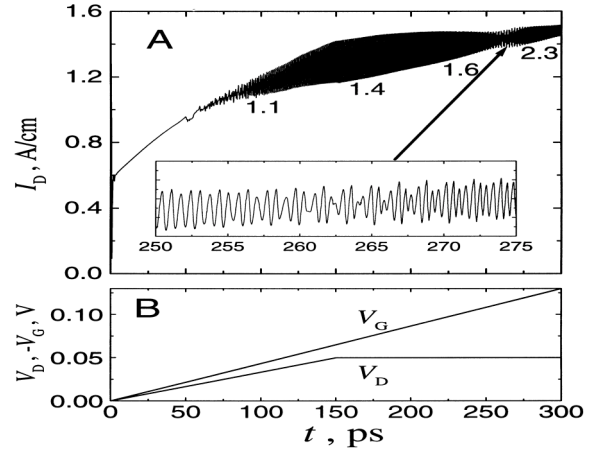


Fig.7. Dependence of FET drain current I_D on gate potential V_G (A). Dependences of gate potential V_G and drain potential V_D on time t (B). Parameters: $l = 0.35 \mu\text{m}$, length of the gate $l_G = 0.28 \mu\text{m}$, $N_0 = 2 \cdot 10^{11} \text{ cm}^{-2}$, $\epsilon_F^{(S)} = 0.035 \text{ eV}$, $\epsilon_F^{(D)} = 0.0175 \text{ eV}$. Other parameters are the same as in Fig.6.

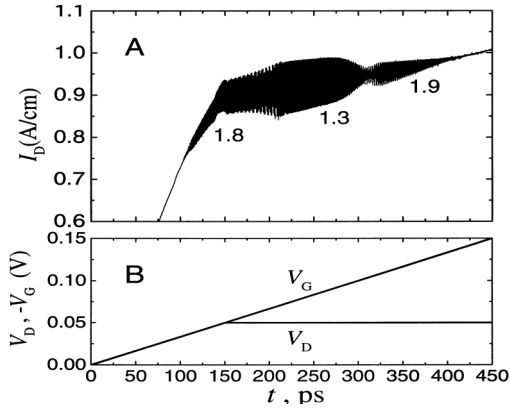


Fig.8. Dependence of FET drain current I_D on gate potential V_G (A). Dependences of gate potential V_G and drain potential V_D on time t (B). Up to $t = 150 \text{ ps}$ both V_D and V_G increase simultaneously. After $t = 150 \text{ ps}$ V_D is constant, and V_G continues to increase. Parameters: $l = 0.4 \mu\text{m}$, $l_G = 0.32 \mu\text{m}$, $N_0 = 2 \cdot 10^{11} \text{ cm}^{-2}$, $\epsilon_F^{(S)} = 0.025 \text{ eV}$, $\epsilon_F^{(D)} = 0.025 \text{ eV}$. Other parameters are the same as in Fig.6.

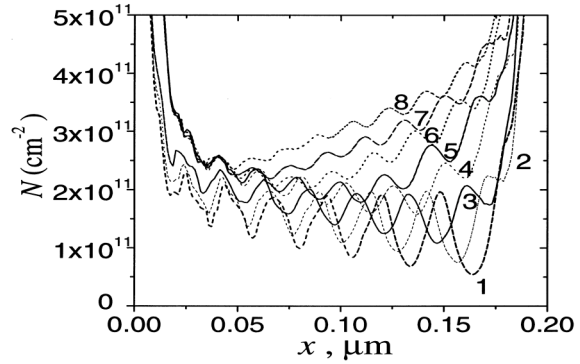


Fig.9. Distribution of electron concentration N in asymmetric ballistic FET for different applied voltages V_D : 0.7 V (1), 0.63 V (2), 0.53 V (3), 0.42 V (4), 0.35 V (5), 0.3 V (6), 0.27 V (7), 0.25 V (8). Parameters: $l = 0.2 \mu\text{m}$, $d = 0.048 \mu\text{m}$, $N_0 = 5 \cdot 10^{11} \text{ cm}^{-2}$, $V_G = -0.03 \text{ V}$. Other parameters are the same as in Fig.6.

References:

1. J. R. Pierce, J. Appl. Phys., **19**, 231 (1948).
2. B. B. Robinson and G. A. Swartz, J. Appl. Phys., **38**, 2461 (1967).
3. G. A. Swartz and B. B. Robinson, J. Appl. Phys., **40**, 4598 (1969).
4. N. A. Bannov, V. I. Ryzhii, and V. A. Fedirko, Sov. Phys. Semicond., **17**, 36 (1983).
5. V. I. Ryzhii, N. A. Bannov, and V. A. Fedirko, Sov. Phys. Semicond., **18**, 481 (1984).
6. E. M. Lifshitz and L. P. Pitaevskii, Physical Kinetics, Oxford, New York, Pergamon Press, 1980.
7. A. A. Sukhanov, V. B. Sandomirskii, and Yu. Yu. Tkach, , Sov. Phys. Semicond., **17**, 1378 (1983).
8. V. V. Mantrov and A. A. Sukhanov, Sov. Phys. Semicond., **19**, 882 (1985).
9. V. E. Gantmakher and Y. B. Levinson, Carrier Scattering in Metals and Semiconductors, North Holland, Amsterdam, 1987.
10. J. R. Eisenstein, Superlatt. & Microstruct., **12**, 107 (1992).